RNA (2002), *8*:188–201. Cambridge University Press. Printed in the USA.

DOI: 10.1017.S135583820101278X

Determinants of the recognition of enteroviral cloverleaf RNA by coxsackievirus B3 proteinase 3C

ROLAND ZELL,[1] KARIM SIDIGI,[1] ENRICO BUCCI,[2,3] AXEL STELZNER,[1] and MATTHIAS GÖRLACH[3]

[1]Institut für Virologie, Klinikum der Friedrich-Schiller-Universität, 07745 Jena, Germany
[2]Centro di Studio di Biocristallografia, 80134 Naples, Italy
[3]Abteilung Molekulare Biophysik/NMR-Spektroskopie, Institut für Molekulare Biotechnologie, 07745 Jena, Germany

ABSTRACT

The initiation of enteroviral positive-strand RNA synthesis requires the presence of a functional ribonucleoprotein complex containing a cloverleaf-like RNA secondary structure at the 5′ end of the viral genome. Other components of the ribonucleoprotein complex are the viral 3CD proteinase (the precursor protein of the 3C proteinase and the 3D polymerase), the viral 3AB protein and the cellular poly(rC)-binding protein 2. For a molecular characterization of the RNA-binding properties of the enteroviral proteinase, the 3C proteinase of coxsackievirus B3 (CVB3) was bacterially expressed and purified. The recombinant protein is proteolytically active and forms a stable complex with in vitro-transcribed cloverleaf RNA of CVB3. The formation of stable complexes is also demonstrated with cloverleaf RNA of poliovirus (PV) 1, the first cloverleaf of bovine enterovirus (BEV) 1, and human rhinovirus (HRV) 2 but not with cloverleaf RNA of HRV14 and the second cloverleaf of BEV1. The apparent dissociation constants of the protein:RNA complexes range from approx. 1.7 to 4.6 μM. An electrophoretic mobility shift assay with subdomain D of the CVB3 cloverleaf demonstrates that this RNA is sufficient to bind the CVB3 3C proteinase. Binding assays using mutated versions of CVB3 and HRV14 cloverleaf RNAs suggest that the presence of structural features rather than a defined sequence motif of loop D are important for 3C proteinase–RNA interaction.

Keywords: CD spectroscopy; enterovirus replication; picornavirus; replication initiation; RNA secondary structures

INTRODUCTION

The 5′ nontranslated region (5′ NTR) of enteroviruses and rhinoviruses contains RNA elements that serve in the initiation of cap-independent translation and in the initiation of positive-strand RNA synthesis (Rueckert, 1995). For poliovirus type 1 (PV1), a cloverleaf-like secondary structure was recognized to be of considerable importance for the latter process. It is part of a ribonucleoprotein (RNP) complex comprising viral and cellular proteins. Formation of 3CD proteinase:cloverleaf RNA complexes in vitro was first described by Andino and coworkers (1990a). It was observed that the precursor protein 3CD proteinase ($3CD^{pro}$) rather than 3C proteinase ($3C^{pro}$) binds with high affinity to the positive-strand RNA cloverleaf of poliovirus (Andino et al., 1993; Harris et al., 1994). Further data support the hypothesis that complex formation with 3AB (a membrane-associated precursor of the VPg peptide) enhances the affinity of $3CD^{pro}$ to RNA (Xiang et al., 1995). Another protein shown to bind in vitro to this RNA is the cellular poly(rC)-binding protein (PCBP) 2 (Andino et al., 1993; Gamarnik & Andino, 1997; Parsley et al., 1997). However, its role in replication initiation is not yet clear and there might be additional downstream elements of the internal ribosomal entry site (IRES) that function in replication (Borman et al., 1994).

In analogy to the paradigmatic poliovirus, it was assumed that interactions of the $3CD^{pro}$ and cloverleaf RNA are also essential for other entero- and rhinoviruses, including coxsackievirus B3 (CVB3). For rhinovirus 14 (HRV14), the interaction of $3C^{pro}$ and the cloverleaf RNA was demonstrated (Leong et al., 1993; Walker et al., 1995). In an in vivo approach, chimeric virus constructs were used to demonstrate that the 5′ cloverleaf and the IRES region are signal structures that function in different viral backgrounds. The viability of virus chimeras with hybrid 5′ NTRs indicates that the

Reprint requests to: Roland Zell, Institut für Virologie, Klinikum der Friedrich-Schiller-Universität, Winzerlaer Str. 10, 07745 Jena, Germany; e-mail: i6zero@rz.uni-jena.de.

$3CD^{pro}$:cloverleaf interaction is not species specific (Johnson & Semler, 1988; Xiang et al., 1995; Zell et al., 1995, 1999; Todd et al., 1997). This suggests that the proteinase precursor may also recognize cloverleaf RNA of other enterovirus species to initiate replication. The cloverleaf-like RNA secondary structure is highly conserved among all enteroviruses and rhinoviruses with the exception of the bovine enterovirus (BEV), which has two cloverleaf-like RNA secondary structures separated from each other by a small stem-loop (Zell & Stelzner, 1997). The 5′ cloverleaf secondary structure contains four subdomains joint by a four-way junction: stem A and the stem-loop subdomains B, C, and D (Fig. 1A). The subdomain D is a stem-loop containing an asymmetric bulge at its base; a symmetric bulge bound by two base-paired stem regions; and an apical loop, the D-loop. The stem and bulge region of subdomain D is highly conserved in sequence, whereas the D-loop is less conserved yet comprises, in most cases, 4 nt (Fig. 1B; Zell & Stelzner, 1997). Three nucleotides are found in the D-loop of rhinovirus 14 and five are found in the D-loop of the second cloverleaf of BEV (Zell & Stelzner, 1997). In vitro data (Andino et al., 1990a; Walker et al., 1995) consistently point towards subdomain D as the RNA ligand for $3C^{pro}$ or $3CD^{pro}$, respectively. The biological significance of this hypothesis is supported by in vivo data of a suppressor mutant (Andino et al., 1990b) and by the viability of chimeric viruses (Johnson & Semler, 1988; Xiang et al., 1995; Zell et al., 1995, 1999; Todd et al., 1997). However, whereas in the case of PV1 it was concluded that the D-loop is a major determinant of specific binding of $3CD^{pro}$, for HRV14, the notion was put forward that the stem region of subdomain D harbors major determinants of specific $3C^{pro}$ binding (Leong et al., 1993; Walker et al., 1995). Considering the deleterious structural effects mutations could have upon either of these regions on the overall structure of subdomain D, we reasoned that it might be useful to address the specific binding of $3C^{pro}$ to subdomain D in more detail. To that end, proteolytically active $3C^{pro}$ from CVB3 was recombinantly expressed, purified, and used for in vitro binding assays employing the 5′ cloverleaves of several entero- and rhinovirus species and mutants thereof. Furthermore, the specificity of binding of $3C^{pro}$ to subdomain D was investigated. The present experiments indicate that it is the number of nucleotides rather than a specific loop sequence in the D-loop that provides a major determinant for specific $3C^{pro}$ binding.

RESULTS

Bacterially expressed $3C^{pro}$ of CVB3 is proteolytically active

The $3C^{pro}$ of PV1 and HRV14 were previously shown to have at least two functional activities: proteolysis of viral and cellular proteins (for a review, see Ryan & Flint, 1997) and binding of cloverleaf RNA (Andino et al. 1990a; Leong et al., 1993). To investigate the RNA-binding properties of the CVB3 $3C^{pro}$, the respective viral gene region was cloned into the pET23a vector, expressed in *Escherichia coli* and purified from bacterial extracts (see Materials and Methods). Briefly, CVB3 $3C^{pro}$ was purified in two steps by ion exchange and gel filtration chromatography according to Nicklin et al. (1988). The purified CVB3 $3C^{pro}$ contained no visible protein contaminants as judged from CBB-stained gels (data not shown).

Recently, human poly(A)-binding protein (PABP; 70.7 kDa, 636 amino acids) was shown to be a natural substrate of the polioviral $3C^{pro}$ (Joachims et al., 1999). To assess the structural integrity of the recombinant purified $3C^{pro}$, its proteolytic activity was tested biochemically. PABP-containing bacterial extracts (Görlach et al., 1994) were mixed with 10 μM purified $3C^{pro}$ and incubated at 37°C for 8 h according to a previously described method (Nicklin et al., 1988). Subsequent SDS polyacrylamide (PAA) gel electrophoresis of the mixture revealed a cleavage product of approximately 60 kDa (data not shown). This fragment corresponds to a calculated 60.4 kDa cleavage product assuming proteolysis at Q_{540}-G_{541} of the human PABP. The circular dichroism (CD) spectrum obtained from the purified proteinase is characteristic of a folded protein and very similar to the reported spectrum for HRV14 $3C^{pro}$ (Wang & Johnson, 2001). Analysis of the CD spectrum gave the secondary structure fraction as reported in Figure 2.

CVB3 $3C^{pro}$ binds to enteroviral and rhinoviral cloverleaf RNAs

In analogy to PV1 and HRV14, it is thought that proteinases from other enteroviruses also bind to cloverleaf RNA. The ability of purified recombinant CVB3 $3C^{pro}$ to form a RNP complex with 5′-cloverleaf RNA was examined by electrophoretic mobility shift assay (EMSA) using in vitro-transcribed cloverleaf RNA from various viruses (Fig. 1A). Cloverleaf RNA (20 μM) was incubated in the presence of increasing concentrations of $3C^{pro}$. The samples were separated on native 10% PAA gels. RNA was stained with ethidium bromide and visualized using UV light. Figure 3A shows a typical result of this experiment. Free CVB3 cloverleaf RNA appears to exist in two conformations as judged from the occurrence of two distinct bands in the absence of proteinase in native PAA gels, whereas the RNA appears as a single band in PAA gels containing 8 M urea (data not shown). The amount of the minor slow migrating form (upper band) differs in various RNA preparations (data not shown). In the presence of purified $3C^{pro}$ the major band of the free RNA disappears and a band representing a slow migrating RNA:protein complex is detected. The presence of $3C^{pro}$ in this complex

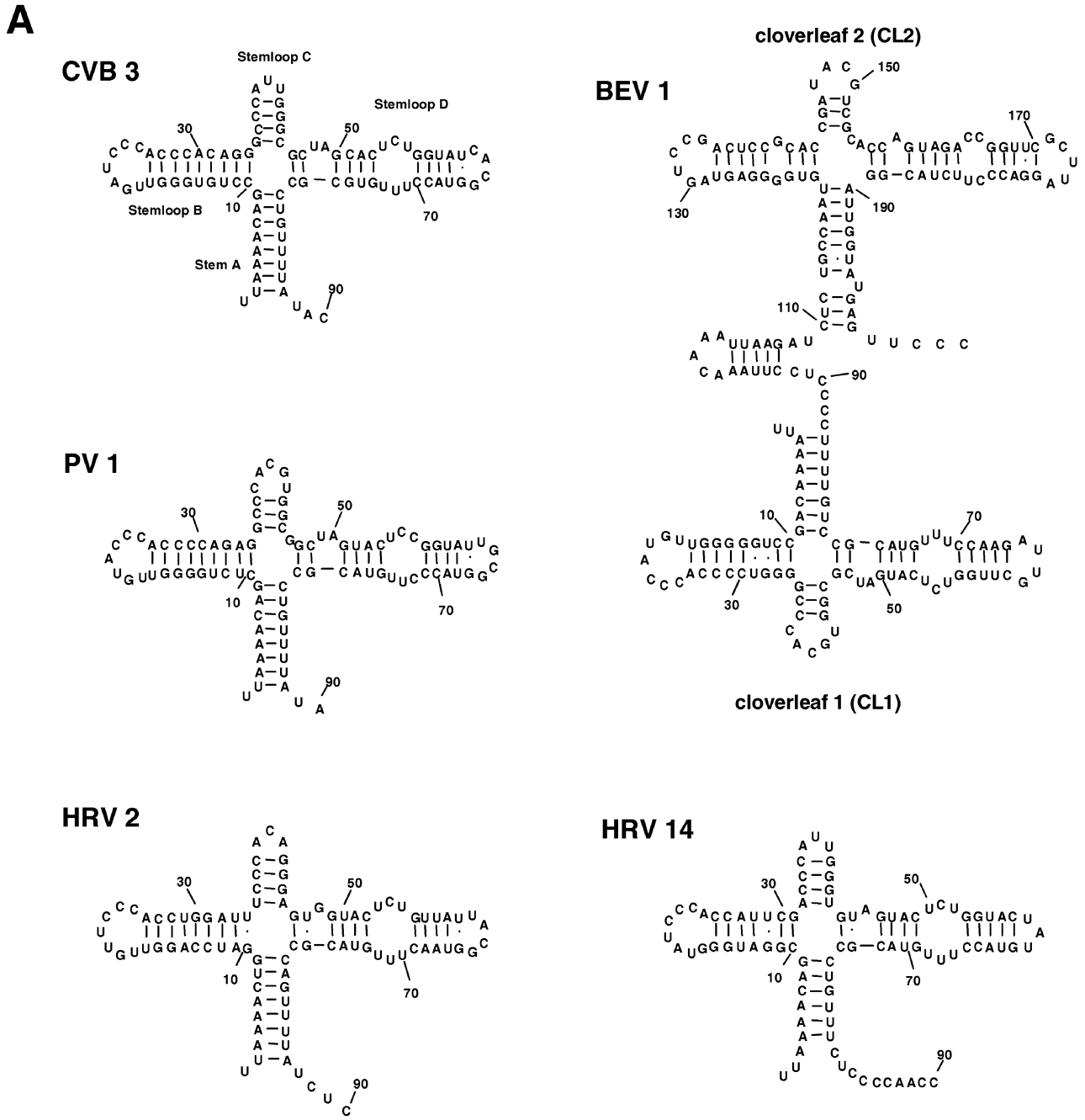

FIGURE 1. *See caption on facing page.*

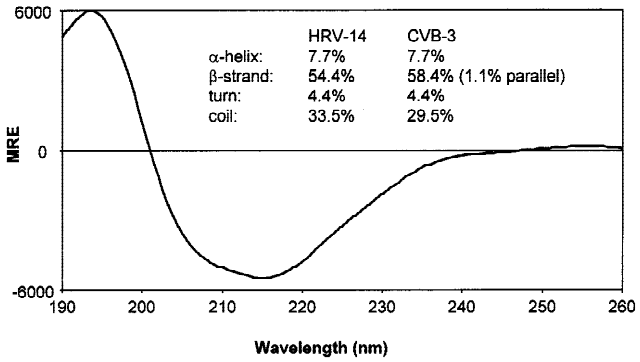

FIGURE 2. Molar ellipticity spectrum of recombinant 3C^{pro} from CVB3. In the inset, the estimated percentages of secondary structure elements are shown in comparison to the corresponding percentages obtained for the known structure of HRV14 3C^{pro} (Matthews et al., 1999). Calculation of the secondary structure content was performed as described in the text.

was subsequently ascertained using CBB staining (Fig. 3A).

To demonstrate the formation of complexes between CVB3 3C^{pro} and heterologous cloverleaf domains, the cloverleaf RNAs of PV1, HRV2, HRV14, and BEV1 were prepared and incubated with recombinant purified CVB3 3C^{pro}. The EMSAs showed complex formation for PV1, HRV2, and RNAs containing the first BEV1 cloverleaf (Fig. 3A). However, complex formation was not observed for the HRV14 cloverleaf and the second cloverleaf of BEV1 (Fig. 3B).

Filter-binding assays were performed to determine the affinity of the recombinant 3C^{pro} for the various cloverleaf RNAs (Fig. 4). Control experiments using HRV14 cloverleaf and BEV1 cloverleaf 2 were included showing binding curves typical for weak and unspecific binding. For the cloverleaves able to specifically bind CVB 3C^{pro}, the apparent dissociation constants (K_d) were determined as the proteinase concentrations at which a 50% saturation of ^{32}P-labeled cloverleaf RNA binding was observed (see Materials and Methods). The apparent K_d ($K_{d,app}$) for the RNAs tested ranged from 1.7 to 4.6 μM.

3C^{pro} specifically binds to stem-loop D of the cloverleaf

In a previous study, the subdomain D of the cloverleaf was suggested to interact with the PV1 3CD^{pro} (Andino et al., 1990a, 1993). Moreover, HRV14 3C^{pro} was shown to interact with a RNA representing the HRV14 subdomain D (Walker et al., 1995). To test whether the CVB3 stem-loop D RNA is sufficient to bind CVB3 3C^{pro}, two RNAs representing an extended stem-loop D (38 nt, Fig. 5A) and a shortened version (30 nt) were in vitro transcribed and incubated with the recombinant proteinase. The EMSA showed complex formation for both RNA molecules (Fig. 5B). The $K_{d,app}$ value of the extended version determined by filter binding assay was 4.6 μM, which is similar to the dissociation constant obtained for the entire cloverleaf RNA (Fig. 4). A fraction of the complexes apparently dissociates during gel analysis, leading to a smear that has a higher molecular weight than the free RNA. This partial dissociation of the complex during the 18-h gel run is probably due to the micromolar affinity of 3C^{pro} for stem-loop D.

To demonstrate the specificity of the stem-loop D:3C^{pro} interaction, CVB3 3C^{pro} was incubated with stem-loop B RNA. In a parallel experiment, human PCBP2 was incubated with stem-loop D RNA. As shown in Figure 5B, 3C^{pro} but not PCBP2, interacts with stem-loop D and PCBP 2 but not 3C^{pro} interacts with stem-loop B, indicating that each protein specifically interacts with its target RNA.

Nucleotides of the loop of subdomain D are important for binding of 3C^{pro}

As subdomain D is sufficient for specific binding of 3C^{pro} to the cloverleaf, EMSAs with cloverleaf RNAs mutated in this subdomain should answer the question whether the loop region contains important elements for the interaction with CVB3 3C^{pro}. To examine this question, three plasmids were constructed that allow the in vitro transcription of mutated cloverleaf RNAs (Fig. 6A): (1) a CVB3 cloverleaf in which nt 64 of the D-loop was deleted (CACG $\rightarrow$ CAG, CVB3-Δ64); (2) a CVB3 cloverleaf in which the loop region of the subdomain D was replaced by the corresponding loop region of HRV14 (CACG $\rightarrow$ UAU, CVB3-HRV14loop); and (3) a mutated HRV14 cloverleaf RNA with an insertion at nucleotide position 60 within the D-loop (UAU $\rightarrow$ UAUG, HRV14-Ins60). The EMSAs using recombinant CVB3 3C^{pro} and the mutated cloverleaf RNAs revealed complex formation in the case of the mutated HRV14 cloverleaf RNA (HRV14-Ins60; Fig. 6B) whereas the mutant

FIGURE 1. (*facing page*) Comparison of enteroviral and rhinoviral cloverleaf RNAs. **A:** The putative 5′ cloverleaves of CVB3, PV1, HRV2, HRV14, and the two cloverleaves of BEV1 are depicted. The folding patterns and the sequences of the cloverleaves are conserved. **B:** Structure of the consensus stem-loop D based on a nucleotide alignment (data not shown) of 60 enteroviral and rhinoviral sequences. Numbers indicate the frequency of the respective nucleotide in percent. For some residues, the next frequent nucleotide is presented in parenthesis. Note, that the loop sequence is significantly less conserved than the stem. The substitution of a G/C base pair by an A/U base pair (boxed) is characteristic for HRV-A serotypes. Also, all rhinoviruses have an asymmetric bulge at the base of stem-loop D (HRV2 nt 49, HRV14 nt 45) consisting of 1 nt instead of 2 as found in enteroviruses.

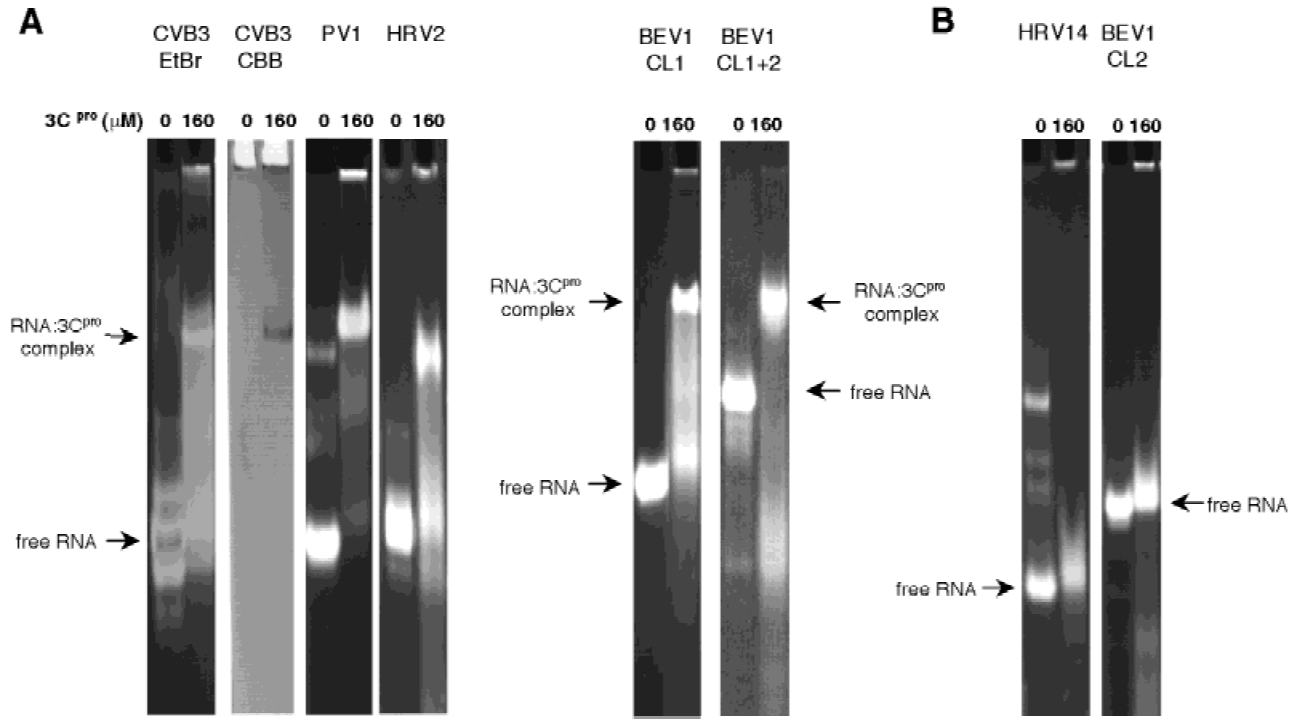

FIGURE 3. EMSAs of cloverleaf RNAs and recombinant 3C^{pro}. **A:** RNAs (20 μM) representing the cloverleaves of CVB3, PV1, HRV2, the first BEV1 cloverleaf (CL1), and both BEV1 cloverleaves (CL1+2) were incubated at room temperature for 15 min in the presence (160 μM) or absence (0 μM) of recombinant CVB3 3C^{pro} and applied to a native 10% PAA gel. After electrophoresis, RNA was stained with ethidium bromide (EtBr) and visualized using UV light. Arrows indicate free RNA and the RNA:3C^{pro} complex. To demonstrate the presence of protein in the complex with the CVB3 cloverleaf, the PAA gel was also stained with Coomassie brilliant blue (CBB). **B:** Cloverleaf RNA (30 μM) of HRV14 and the second cloverleaf (CL2) of BEV1 were incubated with 3C^{pro}.

CVB3 cloverleaves with a tri-loop (CVB3-Δ64; CVB3-HRV14loop) did not bind 3C^{pro}.

CD spectroscopy of cloverleaf RNAs

From the data presented above and from earlier studies (Andino et al., 1990b; Walker et al., 1995) it is clear that subdomain D is the major determinant for 3C^{pro} binding to the 5′ cloverleaf. In addition, the present experiments involving mutant forms of the CVB3 and HRV14 cloverleaves suggest that it is not the sequence of the D-loop but rather the presence of 4 instead of 3 nt within this loop that allows for a specific complex formation. This fact points to an important role of the three-dimensional structure of the D-loop in the binding process and suggests that the D-loop is only bound when it can adopt a correct conformation. In lack of a known three-dimensional structure of subdomain D, CD measurements on the cloverleaf RNAs of CVB3, CVB3-Δ64, HRV14, and HRV14-Ins60 were undertaken to test this hypothesis. After insertion of a G residue into the D-loop of the HRV14 cloverleaf, this RNA is recognized by 3C^{pro} of CVB3. The CD spectra of the two cloverleaves are reported in Figure 7. Remarkable differences are observed in the 250–210 nm region. In a similar experiment, comparison of the wild-type CVB3 cloverleaf with the mutant cloverleaf obtained after elimination of C_{64} from the D-loop also demonstrated CD differences in the region 250–210 nm. Although the spectra of the wild-type CVB3 and the mutant CVB3 cloverleaves are obviously different from the corresponding spectra of wild-type HRV14 and the mutant HRV14 cloverleaves, the spectral difference between the two CVB3 cloverleaf RNAs is remarkably similar to the spectral difference between the two HRV14 cloverleaves (inset of Fig. 7).

DISCUSSION

Interaction of recombinant CVB3 3C^{pro} and in vitro-transcribed cloverleaf RNA is not species specific

The 3C^{pro} of enteroviruses and rhinoviruses and its precursor proteins (3CD^{pro}) are thought to be multifunctional proteins. Beside their proteolytic activity, they specifically recognize the 5′ cloverleaf of the viral positive-strand RNA leading to the formation of a functional RNP complex (Ryan & Flint, 1997). The biologi-

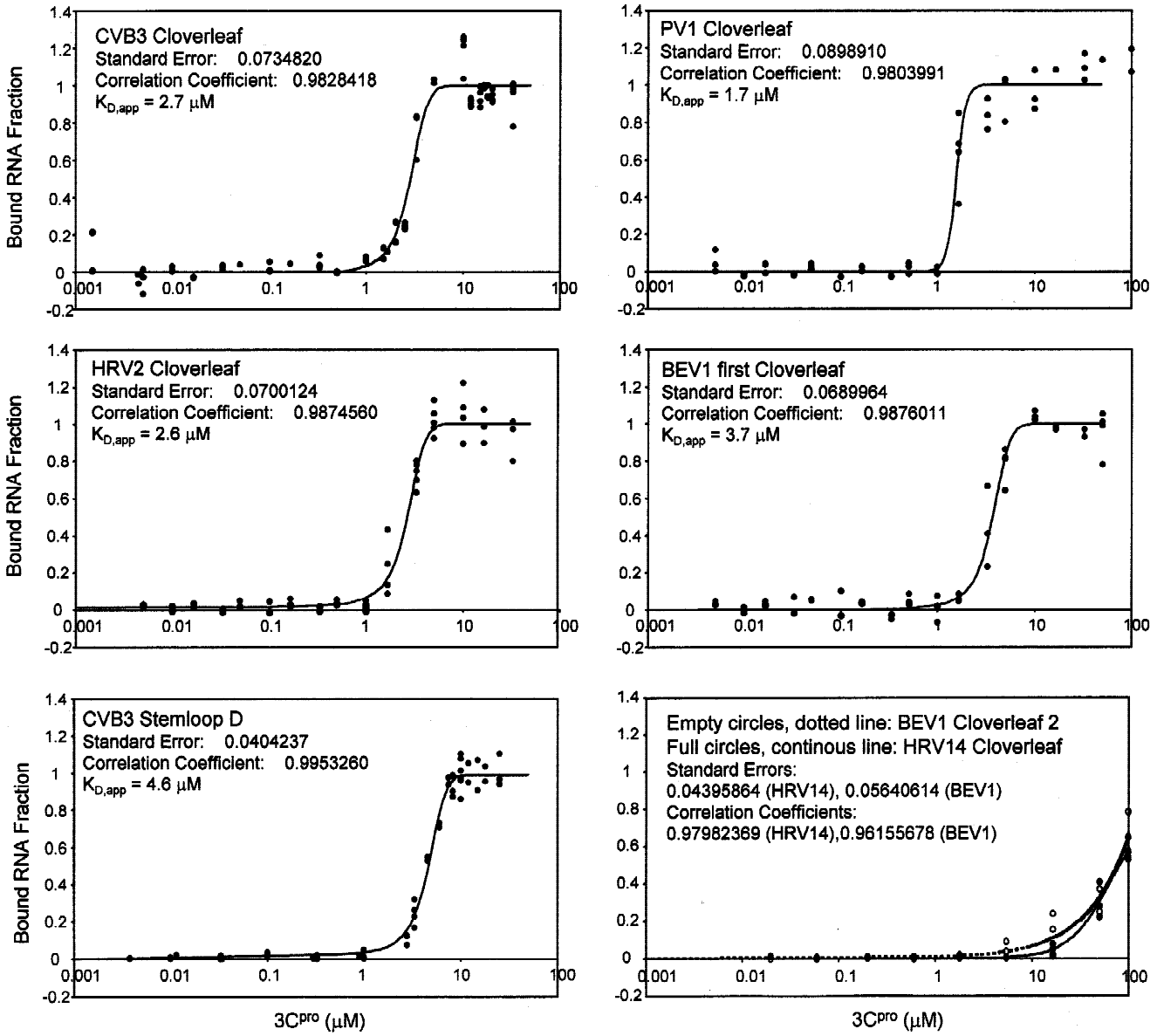

FIGURE 4. Determination of the apparent dissociation constants ($K_{d,app}$) of various RNA:3C^{pro} complexes. To determine the $K_{d,app}$ values, filter-binding assays were performed with 1.25 pmol ^{32}P-labeled RNA and 10 nM–200 ΔM 3C^{pro}. Binding curves were derived fitting the data points from 10 nM up to 50 ΔM of 3C^{pro}. For the estimation of the $K_{d,app}$, see Materials and Methods. BEV1 cloverleaf 2 and HRV14 cloverleaf are included as negative controls.

cal significance of this interaction was provided by the observation that a 4-nt insertion of the PV1 D-loop is suppressed by mutations of the 3C^{pro}-encoding gene region (Andino et al., 1990b). Among the many enterovirus and rhinovirus serotypes, 3C^{pro}/3CD^{pro} affinities for their respective cloverleaf RNAs seem to differ in vitro: whereas the polioviral 3CD^{pro} (probably in complex with viral 3AB; Xiang et al., 1995) and not 3C^{pro} binds to cloverleaf RNA (Andino et al., 1990a), the 3C^{pro} of HRV14 readily interacts with RNA (Leong et al., 1993). In the distantly related hepatitis A virus (a hepatovirus), both 3C^{pro} and 3CD^{pro} bind with similar affinities to 5′ RNA secondary structures (Kusov & Gauss-Müller, 1997). Nucleotide alignments of all available enteroviral and rhinoviral sequences revealed a highly conserved potential RNA secondary structure element. In this context, the second BEV cloverleaf is a special case, as its nucleotide sequence—with the exception of subdomain D—has no homology to the first cloverleaf (Zell & Stelzner, 1997). The conservation of these structures suggests that very similar interactions within the RNP complex might occur in all of these viruses. This view is supported by the viability of chimeric viruses with heterologous cloverleaves (Johnson & Semler, 1988; Zell et al., 1995, 1999; Todd et al., 1997; Xiang et al., 1995).

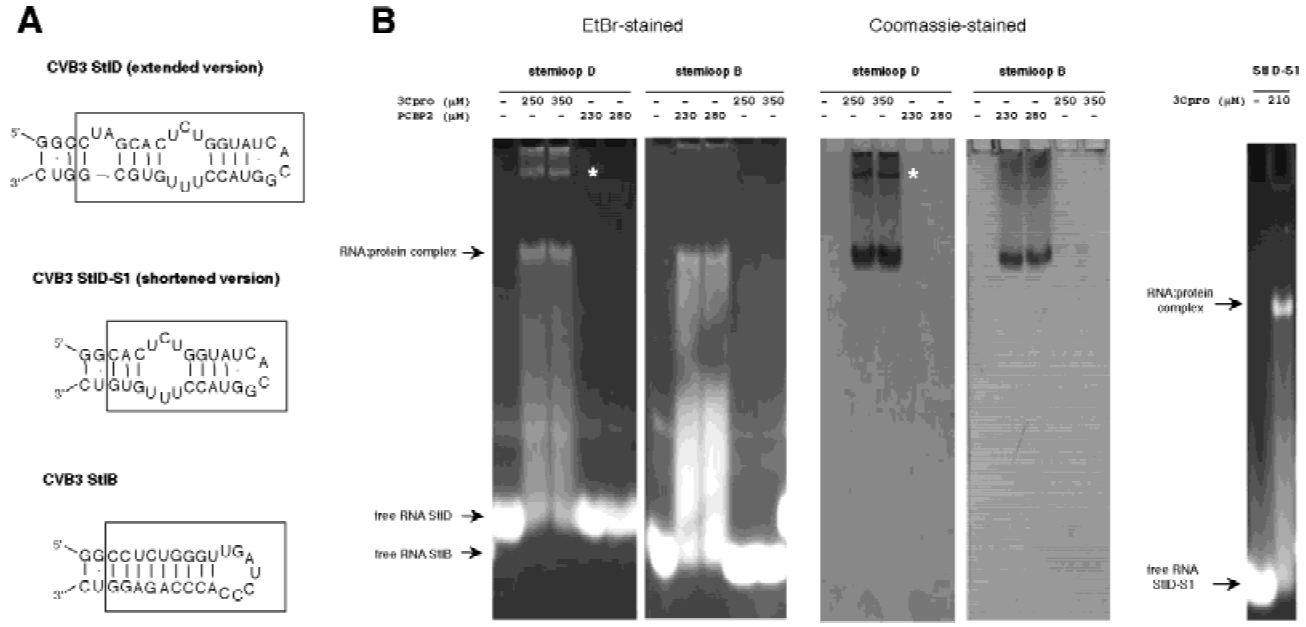

FIGURE 5. EMSA of stem-loops D and B RNAs and recombinant $3C^{pro}$. **A:** RNA molecules representing the extended or shortened version of the CVB3 stem-loop D and the CVB3 stem-loop B. The extended version of stem-loop D includes the asymmetric bulge that is characteristic of all known cloverleaf structures. Boxed nucleotides represent wild-type viral RNA sequences. Additional base pairs at the base of the stem-loops were introduced to achieve efficient T7 transcription and cleavage at the 3′ ends by a hammerhead ribozyme in *cis*. **B:** Interaction of stem-loop D RNAs (50 μM) and stem-loop B RNA (50 μM) with recombinant $3C^{pro}$ and PCBP2, respectively. Arrows indicate free RNA and the RNA:$3C^{pro}$ complexes. Note that an additional, slowly migrating band of stem-loop D RNA induces a second RNP complex. The amount of this band varies in different RNA preparations. $*$ indicates a second RNA:protein complex.

The subdomain D, a region of the cloverleaf known to be involved in the binding of $3CD^{pro}$ in PV1 or $3C^{pro}$ in HRV14 (Andino et al., 1990b; Walker et al., 1995), contains a considerable number of nucleotide substitutions within its apical loop, the D-loop. A comparison of 60 enteroviral and rhinoviral cloverleaf sequences revealed 17 different D-loop sequences (Fig. 1; data not shown). Hence, the question arises whether the conserved stem or the variable D-loop interacts with the $3C^{pro}$/$3CD^{pro}$. The conservation of the stem regions in the subdomain D and the localization of the most differences in the D-loop suggested a simple mechanism to achieve the specific recognition between the RNA and the protein in the cloverleaf:$3C^{pro}$ complex: while the stem region provides the scaffold of the overall RNA structure, the specificity is due to the D-loop sequence. However, the interpretation of previous in vivo and in vitro results led to the seemingly puzzling notion that the stem region as well as the D-loop are the (mutually exclusive) necessary and sufficient major determinants for specific RNA binding by $3CD^{pro}$ or $3C^{pro}$, respectively. In particular, in PV1, the D-loop appeared to be the major determinant because an insertion of an additional 4 nt in the D-loop was complemented by mutations in the $3CD^{pro}$ (Andino et al., 1990b). In contrast, disrupting the stem region of HRV14 subdomain D precluded $3C^{pro}$ binding, whereas mutations in the D-loop or the internal symmetric bulge, respectively, did not significantly affect $3C^{pro}$ binding in vitro (Walker et al., 1995). Together, these data clearly provided evidence for the important role of subdomain D in specific binding of $3CD^{pro}$ or $3C^{pro}$, yet the underlying mechanism of specific RNA binding is not clear. Hence, a more detailed study on the RNA-binding properties of $3C^{pro}$ should help to contribute to the solving of that question.

The RNA-binding activity of the CVB3 $3C^{pro}$ in the presence of different enterovirus cloverleaves was examined. The proteolytically active recombinant proteinase binds to cloverleaf RNA of CVB3 (Fig. 3A). Moreover, the binding of $3C^{pro}$ to both the extended and the shortened version of subdomain D demonstrates that this subdomain is sufficient for the interaction (Fig. 5), just as in the case reported for HRV14 (Walker et al., 1995). Interestingly, CVB3 $3C^{pro}$ also binds to the cloverleaves of PV1, HRV2, and BEV1 (Fig. 3A). However, no binding was observed with cloverleaf RNA of HRV14 and the second cloverleaf of BEV1 (Fig. 3B). The recognition of some cloverleaves with very different D-loop sequences by CVB3 $3C^{pro}$ is in close analogy to the recognition of different loop mutants by HRV14 $3C^{pro}$ (Walker et al., 1995), implying that the loop sequence itself is not related to the specificity of the process. Finally, the absence of binding of

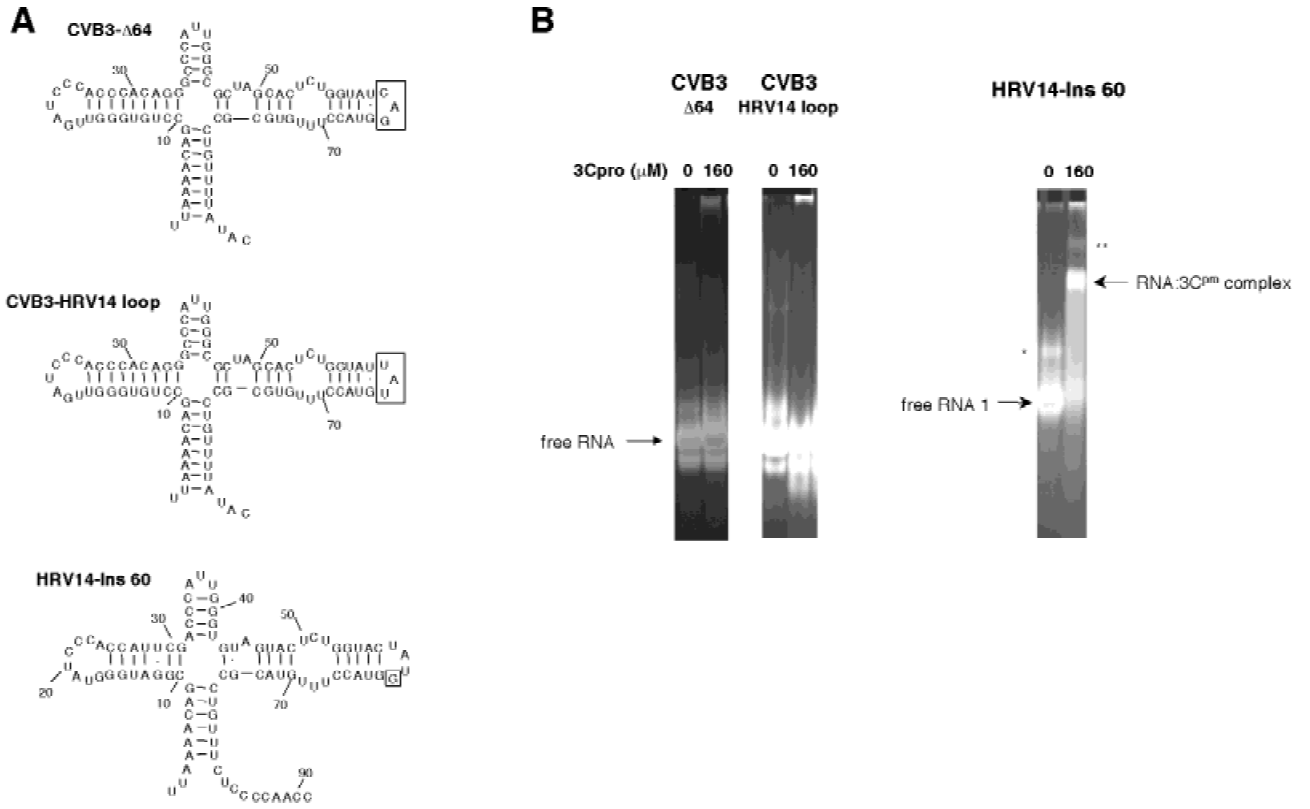

FIGURE 6. Binding of the 3C^{pro} to the loop region of subdomain D. **A:** RNA molecules representing (1) the mutated CVB3 cloverleaf with a deletion of nt 64 (CVB3-Δ64), (2) the mutated CVB3 cloverleaf with a HRV14 D-loop (CVB3-HRV14 loop), and (3) the mutated HRV14 cloverleaf with an insertion at nucleotide position 60 (HRV14-Ins60). The mutated D-loops of the CVB3 cloverleaves and the inserted nucleotide of the HRV14 cloverleaf RNA are boxed. **B:** EMSAs of the mutated cloverleaf RNAs (20 μM) and recombinant 3C^{pro} (160 μM). Left panel: No complex formation is observed with CVB3-Δ64 and CVB3-HRV14 loop RNA. Right panel: Complex formation of a HRV14 cloverleaf RNA with an insertion at nucleotide position 60. ∗ indicates free RNA with a second conformation; ** indicates a minor second RNA:protein complex.

CVB3 3C^{pro} to CVB3-Δ64 clearly shows that the loop region of subdomain D is an important element for complex formation (Fig. 6).

The number of nucleotides of the D-loop influences 3C^{pro} binding by changing the local RNA structure

A comparison of the cloverleaf sequences of CVB3 and HRV14 reveals substitutions at positions 51, 61, and 76 of the base-paired stem of subdomain D and a completely different loop region (see Fig. 1A). EMSAs demonstrate that complexes of cloverleaf RNAs and CVB3 3C^{pro} are formed with RNAs showing a tetra-loop in subdomain D (CVB3, PV1, HRV2, first cloverleaf of BEV1, HRV14-Ins60) but not RNAs with a tri-loop (HRV14, CVB3-Δ64) or a penta-loop (second cloverleaf of BEV1; see Figs. 3 and 6). The existence of some unrecognized cloverleaves means that the proteinase does discriminate certain D subdomains from others. We found this discrimination to be dependent on the loop. The most striking evidence for this fact is the impaired complex formation between CVB3 3C^{pro} and CVB3-Δ64 or CVB3-HRV14loop (Fig. 6). In these cases, the one-base shortening of the loop, whether the other three bases are preserved or not, has a strong effect on the binding. The effect of the D-loop length prompts us to assume a major role for the D-loop structure instead of its sequence in the complex formation process. In particular, those loop sequences that impair 3C^{pro} binding, that is, the two shortened sequences (HRV14, CVB3-Δ64) and the longer penta-loop sequence (BEV1 cloverleaf 2), act possibly through modification of the local RNA structure that is recognized by the protein. This, of course, does not exclude that a particular loop with five or even more nucleotides might adopt a structure that can be recognized by 3C^{pro}. As a matter of fact, there is at least one example of mutation of a RNA octa-loop into an tetra-loop not affecting its binding by a protein, because the recognized structure is preserved in both RNAs(Mirmira & Tinoco, 1996).

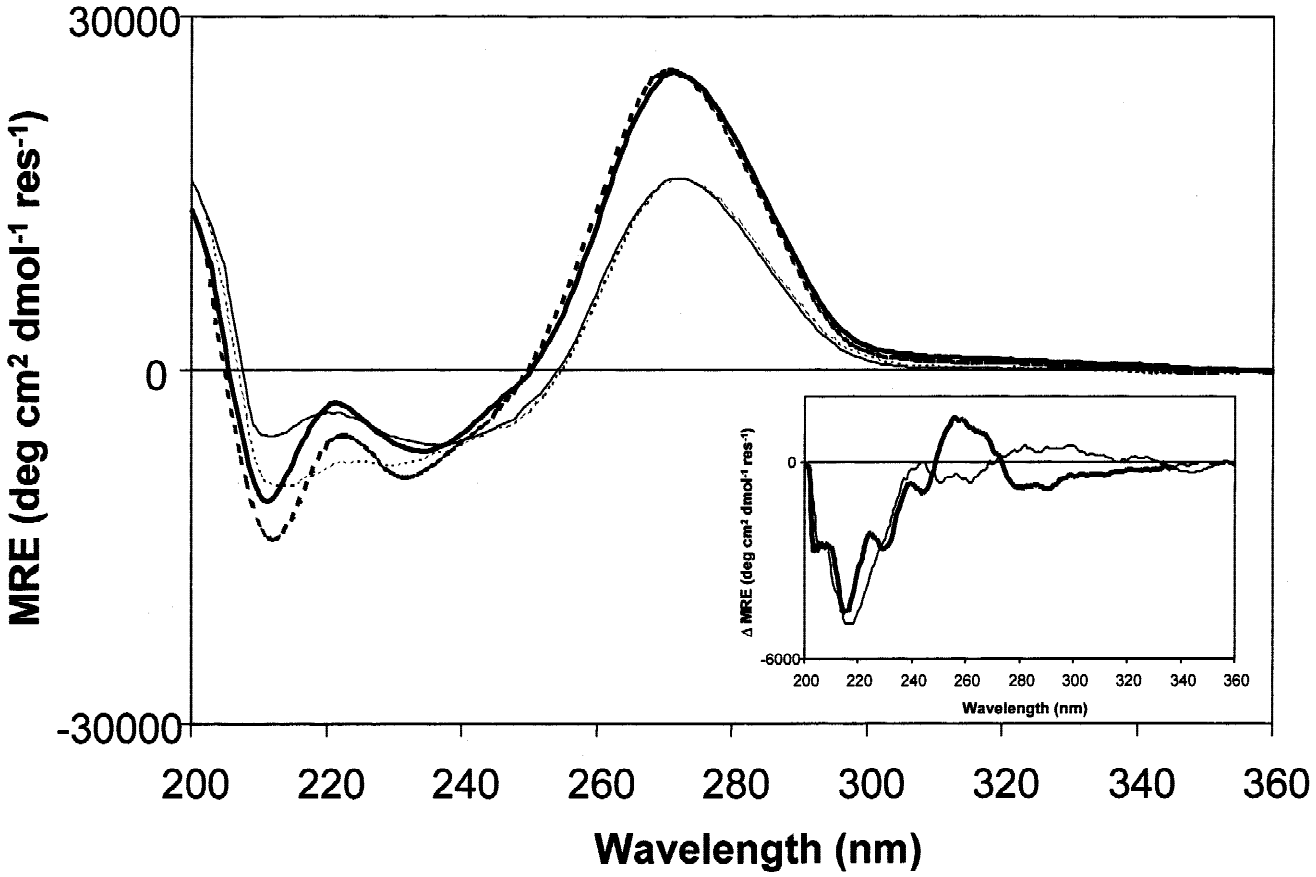

FIGURE 7. CD spectroscopy. CD spectra of wild-type HRV14 (thin continuous line), HRV14-Ins60 (thin dotted line), wild-type CVB3 (bold dotted line), and CVB3-Δ64 (bold continuous line) cloverleaves. Inset: Difference CD spectra between the two CVB3 (bold line) and the two HRV14 (thin line) cloverleaves. All CD spectra are reported as mean molar ellipticity per residue.

CD spectra reveal conformational changes of mutant cloverleaf RNAs

According to the above described hypothesis, one would expect that those stem-loops that are able to bind $3C^{pro}$ differ significantly in structure with respect to binding-impaired stem-loops. Moreover, if $3C^{pro}$ binds a single structure, one may assume that this structure is similar in HRV14-Ins60 and CVB3 (the recognized cloverleaves). To test these predictions, CD experiments on wild-type HRV14, HRV14-Ins60, wild-type CVB3, and CVB3-Δ64 were performed. As described in the Results section, the CD spectra of the two HRV14 cloverleaves (HRV14, HRV14-Ins60) and also the CD spectra of the two CVB3 cloverleaves (CVB3, CVB3-Δ64) exhibit characteristic differences. In both cases, the observed differences between the tri-loop and the tetra-loop versions are not simply due to the addition of a new chromophore (the hetero-aromatic rings of G_{60} or C_{64}), because a G should cause a positive increase at 214 nm and a C should cause an even bigger positive increase at 260 nm (Sprecher & Johnson, 1977). Instead, a major negative increase is always observed at 214 nm and no important changes are observed at 260 nm (Fig. 7, inset). Moreover, the observed changes cannot be explained by the loss or the introduction of a GC base pair, which would cause important changes at 202 nm, nor are they consistent with the loss or the introduction of a canonical AU base pair, which would cause similar changes in the CD spectra (Johnson et al., 1990). As a consequence, the observed changes suggest the reorganization of some noncanonical region of the structure, probably the D-loop, and should involve the appearance and/or disappearance of noncanonical interactions between bases in this region. It is noteworthy that the difference observed in the CD spectra of the two CVB3 RNAs is remarkably similar to the CD difference between the two HRV14 RNAs, even if the inserted or deleted bases are different in the two cases. This fact suggests that in HRV14 and CVB3 cloverleaves, the absence of a single base in the loop (being it a G or a C, respectively) causes, at a first approximation, similar structural changes, when going from a tetra-loop cloverleaf (wild-type CVB3, HRV14-Ins60) to

a tri-loop cloverleaf (CVB3-Δ64, wild-type HRV14). These changes take place regardless of the rest of the cloverleaf or the sequence of the loop.

The observed differences in the CD spectra correlate with the loss or gain of the ability to bind the CVB3 $3C^{pro}$. This observation implies that the CVB3 proteinase recognizes a structure not adoptable by a D-loop consisting of 3 nt only (Leong et al., 1993; Walker et al., 1995). In contrast, $3C^{pro}$ from HRV14 binds to a D-loop, which contains 3 nt (Huang et al., 2001).

Specific binding and low sequence conservation

The low significance of the D-loop sequence in the binding process is mirrored by the lack of any consistent pattern of conservation for three $3C^{pro}$ amino acids (position 144 to 146) that were considered to be important for binding, that is, the complementation of a D-loop mutant in vivo (Andino et al., 1990b). As a matter of fact, if there is not a sequence-to-sequence code recognition between a given subdomain D and its cognate $3C^{pro}$, then the recognition of a four-membered loop is not necessarily correlated with the conservation of those positions within $3C^{pro}$. Moreover, a given $3C^{pro}$ should be able to recognize the structure of a D-loop whenever it can adopt a suitable conformation irrespective of its viral source. Supporting this idea, our data actually show that CVB3 $3C^{pro}$ recognizes in vitro the cloverleaves of CVB3, PV1, HRV2, and BEV1 (Fig. 3), whereas the respective cognate viral proteins are not conserved in the three amino acid positions mentioned above (Fig. 8, upper panel). Importantly, this interpretation is consistent with the observation of viable virus chimeras (Johnson & Semler, 1988; Xiang et al., 1995; Zell et al., 1995, 1999; Todd et al., 1997).

Furthermore, the discrimination between certain D-loops by CVB3 $3C^{pro}$ demonstrated here (Fig. 3 and Fig. 8, middle panel) provides evidence that the KFRDI-motif, which is identical in CVB3 and HRV14 proteinases, does not govern the specific recognition of the D-loop, albeit it is important for RNA binding (Hämmerle et al., 1992; Andino et al., 1993; Leong et al., 1993; Walker et al., 1995). Our model, that $3C^{pro}$ recognizes a structure rather than a sequence of the D-loop, provides a rational for the RNA:$3C^{pro}$ interaction as observed here and by others (Andino et al., 1990a; Leong et al., 1993; Walker et al., 1995), including the discrimination between stem-loops B and D (Fig. 5) and between the mutants of stem-loop D in the context of the entire CVB3 cloverleaf (Fig. 6). The observed lack of species specificity does not pose a major obstacle to rationalize the evolution of such a system. A degree of specificity suffices that ensures that $3C^{pro}$ or $3CD^{pro}$, respectively, can discriminate between its cognate stem-loop D and other elements of the viral RNA or cellular RNAs. Yet, only a three-dimensional structure determination of the entire subdomain D will provide further insight into the basis of RNA–protein interaction in the subdomain D:$3C^{pro}$ complex.

MATERIALS AND METHODS

Plasmid construction, expression, and purification of recombinant coxsackievirus B3 proteinase 3C

For expression plasmid construction, cDNA of the $3C^{pro}$ encoding genome region was amplified using the oligonucleotides 3C-F and 3C-B-stop (see Table 1) and plasmid pCVB3-M2 as template DNA (Lindberg et al., 1992). The PCR fragment corresponding to the reading frame of CVB3 $3C^{pro}$ terminated by a stop codon was *Nde*I-*Xho*I digested and ligated to the *Nde*I-*Xho*I fragment of expression plasmid pET23a(+) (Novagen, Madison, Wisconsin) to yield plasmid pET23a-3Cstop. The structural intactness of this plasmid was verified by DNA sequencing. For expression, *E. coli* strain BL21 (DE3) transformed with pET23a-3Cstop was grown at 37 °C. At 0.5 OD_{595}, expression was induced by adding 0.5 mM isopropyl-β-D-thiogalactopyranoside (IPTG). After incubation for 3 h at 37 °C, the cells were harvested, resuspended in buffer A (40 mM Tris-HCl, pH 7.9, 100 mM NaCl, 15 mM mercaptoethanol), and lysed with a french press (3 cycles at 1,000 psi). The lysate was clarified by centrifugation at 17,500 rpm (4 °C) for 20 min. The $3C^{pro}$ was purified using a modified procedure according to Nicklin and coworkers (1988). Briefly, the $3C^{pro}$-containing supernatant was precipitated by ammonium sulfate (60% at 4°C) and the pellet was resuspended in buffer AB (30 mM Tris-HCl, pH 7.9, 50 mM NaCl, 50 mM KCl, 5 mM $MgCl_2$, 0.5 mM EDTA, 15 mM mercaptoethanol). After dialysis against buffer AB, the protein was applied to DEAE sepharose in buffer B (20 mM Tris-HCl, pH 7.9, 100 mM KCl, 10 mM $MgCl_2$, 1 mM EDTA, 15 mM mercaptoethanol) and unbound fractions were collected, dialyzed against buffer C (20 mM potassium acetate, pH 6.0, 100 mM KCl, 15 mM mercaptoethanol) and loaded onto a sephacryl SH200 column in buffer C. $3C^{pro}$-containing unbound fractions were pooled and concentrated in Centriprep/Centricon spin concentrators (Amicon) up to a concentration of 5 mg/mL to yield highly purified $3C^{pro}$.

Plasmid construction, expression, and purification of recombinant human poly(rC)-binding protein 2

The cDNA of the poly(rC)-binding protein (PCBP) 2 of pQE30 (gift of E. Ehrenfeld, National Institutes of Health, Bethesda, Maryland, USA; Blyn et al., 1995) was cloned into the *Bam*HI-*Pst*I-digested pQE9 (Qiagen, Hilden, Germany) and sequenced to verify structural intactness. Growing *E. coli* JM109 transformed with pQE9-PCBP2 were induced with IPTG at OD_{600} 0.5 and harvested after 17 h of expression at ambient temperature. The his-tagged recombinant protein was purified using Ni-NTA agarose according to the manufacturer's description (Qiagen, Hilden, Germany).

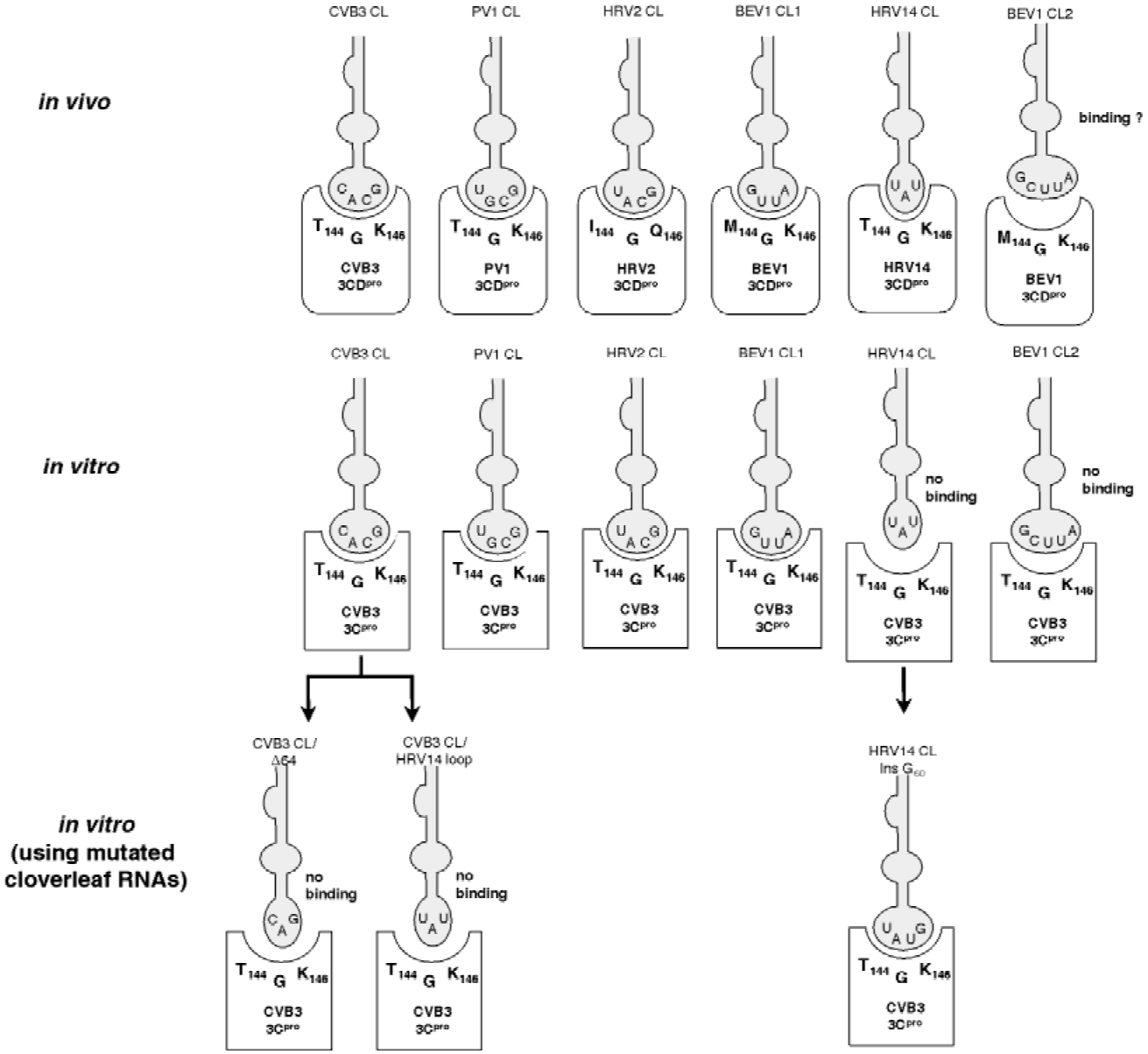

FIGURE 8. Cloverleaf RNA:proteinase interactions. Upper panel: It is generally accepted that in enteroviruses and rhinoviruses RNA:protein interactions of $3CD^{pro}$ and cloverleaf RNA give rise to a functional replication initiation complex in vivo although this was only shown for poliovirus. For rhinovirus, a cloverleaf RNA:$3C^{pro}$ complex was demonstrated in vitro. It is also supposed that the conserved sequence KFRDI (not shown) and the amino acids 144–146 of the PV1 $3C^{pro}$ moiety (as indicated) are involved in binding to the loop region of subdomain D. These three amino acids are not conserved among the entero- and rhinoviruses. Middle panel: In vitro, CVB3 $3C^{pro}$ interacts with several cloverleaf RNAs presenting a tetra-loop in subdomain D. The cloverleaf of HRV14 and the second cloverleaf of BEV1 are not bound. The loop sequence appears to have no influence on binding affinity. Lower panel: The presence of a tetra-loop in subdomain D of HRV14-Ins60 rather than a conserved nucleotide sequence of the remaining cloverleaf is an important determinant for stable complex formation in vitro.

Plasmid construction, in vitro transcription, and purification of enteroviral and rhinoviral cloverleaf RNAs

For cloning of enteroviral and rhinoviral cloverleaf-encoding genome regions, DNA fragments from plasmids pCVB3-M2, pPV16 (gift of E. Wimmer, State University of New York at Stony Brook, New York, USA), pGem-3Z-BEV1 (gift of E. Hoey, Queen's University, Belfast, United Kingdom), and pHRV2 (gift of T. Skern, University of Vienna, Austria) were amplified using the oligonucleotides CVB-Eco, CVB-Bam, PV-Eco, PV-Bam, BEV-CL1-Eco, BEV-CL1-Bam, BEV-CL2-Eco, BEV-CL2-Bam, HRV2-Eco, and HRV2-Bam, respectively (see Table 1). For cloning of the HRV14 cloverleaf, RNA from HRV14-infected HeLa cells was reverse transcribed and the cDNA was amplified using the oligonucleotides HRV14-Eco and HRV14-Bam. The oligonucleotide primers were designed to fuse the T7 promoter 5′ to the cloverleaf-encoding se-

TABLE 1. Oligonucleotides.

Primer designation	Sequence
3C-F[a]	5′-GGAGATATA**CAT***ATG*GGCCCTGCCTTTGAGTTCGCCGTC-3′
3C-B-stop[b]	5′-CATCGG**CTCGAG***CTA*TTGCTCATCATTGAAGTAGTGTTTGAGGAG-3′
CVB-Eco[c]	5′-GATCTA**GAATTC***TAATACGACTCACTATA*GGTTAAAACAGCCTGTGGGTTG-3′
CVB-Bam[d]	5′-GATCTA**GGATTC**AGTTGGGGGAGGGGGTATA-3′
Rsa-HRV-1[e]	5′-GATCTA**GTAC**AATATACCAGAGTGCTAGCGCCCAAT-3′
Rsa-HRV-2[e]	5′-ATCACG**GTAC**CTTTGTGCGCC-3′
CVB-Kpn-Δ64[f]	5′-GATCTA**GGTACC**TGATACCAGAGTGCTAGCGCCCAAT-3′
PV-Eco[c]	5′-GATCTA**GAATTC***TAATACGACTCACTATA*GGTTAAAACAGCTCTGGGGTTGTAC-3′
PV-Bam[d]	5′-GATCTA**GGATTC**TAAAACAGGCGTACAAGGGTAC-3′
BEV-CL1-Eco[c]	5′-GATCTA**GAATTC***TAATACGACTCACTATA*GGTTAAAACAGCCTGGGGGTTGTACC-3′
BEV-CL1-Bam[d]	5′-GATCTA**GGATTC**AAAACAGGCGTACAAAGGTTCTAACG-3′
BEV-CL2-Eco[c]	5′-GATCTA**GAATTC***TAATACGACTCACTATA*GGCTCTGCCAATGTGGGGAGTAG-3′
BEV-CL2-Bam[d]	5′-GATCTA**GGATCC**CTCATACCAATCCGTAGAAGG-3′
HRV2-Eco[c]	5′-GATCTA**GAATTC***TAATACGACTCACTATA*GGTTAAAACTGGATCCAGGTTGTTCC-3′
HRV2-Bam[d]	5′-GATCTA**GGATCC**TAAAACTGGCGTACAAAGTTACCGTAA-3′
HRV14-Eco[c]	5′-GATCTA**GAATTC***TAATACGACTCACTATA*GGTTAAAACAGCGGATGGGTATCCCA-3′
HRV14-Bam[d]	5′-GATCTA**GGATCC**GAAACAGGCGTACAAAGGTACATAGT-3′
Kpn-HRV-1[f]	5′-GATCTA**GGTACC**ATAGTACCAGAGTACTACACCCAA-3′
Kpn-HRV-2[f]	5′-TACTAT**GGTACC**TTTGTACGCC-3′
STLD-HH-F[c]	5′-CCG**GAATTC***TAATACGACTCACTATA*GGCCTAGCACTCTGGTATCACGGTACCTTTGTGC-3
STLD-HH-R[d]	5′-CGC**GGATCC**TTTGTGCGGTTTCGTCCTCACGGACTCATCAGG-3′
STLD-HH-T	5′-CTCTGGTATCACGGTACCTTTGTGCGGTCGGTCCTGATGAGTCCGTGAGGACG-3′
STLD-S1-HH-F[c]	5′-CCG**GAATTC***TAATACGACTCACTATA*GGCACTCTGGTATCACGGTACCTTTGTGTCG-3′
STLD-S1-HH-R[d]	5′-CGC**GGATCC**TTTGTGTTTCGTCCTCACGGACTCATCAGGACGG-3′
STLD-S1-HH-T	5′-GTATCACGGTACCTTTGTGTCGACGGATGTGCTTTCCGTCCTGATGAGTCCGTGAGG-3′
CVB3-B-HH-F[c]	5′-CC**GAATTC***TAATACGACTCACTATA*GGCCTGGGTTGATCCCACCCACAGGTC-3′
CVB3-B-HH-R[d]	5′-CGC**GGATCC**CCACAGGTTTCGTCCTCACGGACTCATCAGG-3′
CVB3-B-HH-T	5′-CCTGGGTTGATCCCACCCACAGGTCGACGGATGTGCTTTCCGTCCTGATGAGTCCGTGAGGACG-3′
Rev. seq. primer	5′-AGCGGATAACAATTTCACACAGGA-3′

[a]Printed in bold and underlined: *Nde*I restriction site; printed in italics: start codon.
[b]Printed in bold and underlined: *Xho*I restriction site; printed in italics: stop codon.
[c]Printed in bold and underlined: *Eco*RI restriction site; printed in bold and italics: T7 promoter.
[d]Printed in bold and underlined: *Bam*HI restriction site.
[e]Printed in bold and underlined: *Rsa*I restriction site.
[f]Printed in bold and underlined: *Kpn*I restriction site.

quence. All PCR fragments were digested with *Eco*RI and *Bam*HI and ligated into the *Eco*RI-*Bam*HI sites of pUC19. The plasmid constructs were sequenced to verify the intactness of nucleotide sequences. For in vitro transcription, approximately 100 μg *Bam*HI-linearized template DNA (200 nM) were incubated for 3–6 h at 37 °C with 70 μg T7 polymerase in a volume of 1 mL transcription buffer (200 mM Tris-Glu, 20 mM DTT, 2 mM spermidine, 25 mM magnesium acetate, and 6 mM of each rNTP, pH 8.1; Grüne et al., 1996). Four to six micrograms of RNA were separated from template DNA on 15% PAA urea (7 M) gels and electroeluted using a S&S BIOTRAP according to the manufacturer's instructions (Schleicher and Schuell, Dassel, Germany).

For the preparation of mutated cloverleaf RNAs, plasmids pUC19-CVB3-Δ64, pUC19-CVB3-CL-HRV14loop, and pUC19-HRV14-CL-Ins60 were constructed using PCR mutagenesis. For this purpose, the oligonucleotide primer pairs CVB-Eco and CVB-Kpn-Δ64, CVB-Eco and Rsa-HRV-1, Rsa-HRV-2 and reverse sequencing (rev. seq.) primer, HRV14-Eco and Kpn-HRV-1, Kpn-HRV-2 and rev. seq. primer (Table 1), were used to generate mutated PCR fragments that were digested with the appropriate enzymes and ligated into the pUC19 polylinker. Mutated cloverleaf RNAs were transcribed and purified as described above.

Plasmid construction, in vitro transcription, and purification of stem-loop D and stem-loop B RNA

For cloning of extended and shortened stem-loop D RNAs of CVB3, the respective DNAs were amplified using the oligonucleotides STLD-HH-F, STLD-HH-R, STLD-S1-HH-F, and STLD-S1-HH-R as PCR primers and the oligonucleotides

STLD-HH-T and STLD-S1-HH-T as templates, respectively (see Table 1). Stem-loop B of the CVB3 cloverleaf was cloned using the oligonucleotides CVB3-B-HH-F, CVB3-B-HH-R, and the template CVB3-B-HH-T. The PCR fragments were digested with *Eco*RI and *Bam*HI and ligated into a *Eco*RI-*Bam*HI fragment of pUC19. All plasmid constructs were sequenced to verify correct nucleotide sequences. In vitro transcription was performed as described above. Primers and templates for the PCR were designed to include a hammerhead ribozyme activity into the in vitro transcribed RNA to ensure homogeneous 3′ ends of the stem-loop RNAs after self-cleavage (Stoldt et al., 1998). After in vitro transcription and autocatalytic cleavage, the RNA molecules representing stem-loop D RNA and stem-loop B RNA, respectively, were separated and electroeluted from 10% PAA urea gels.

Proteinase activity assay

Proteolytic activity was assayed (according to Nicklin et al., 1988) using PABP as substrate (Joachims et al., 1999). Bacterial expression of this protein was previously described (Görlach et al., 1994). Crude extracts of PABP-overexpressing bacteria were incubated in the presence or absence of purified $3C^{pro}$ (10 μM) for 8 h at 37 °C and analyzed with SDS-PAGE.

Electrophoretic mobility shift assay

Purified in vitro-transcribed RNA (20 or 50 μM in buffer C) and $3C^{pro}$ and/or human PCBP2 at increasing final concentrations of 20–350 μM, as given in the corresponding figure legends, were mixed and incubated in a volume of 20 μL buffer C for 15 min at room temperature to allow for complex formation. Subsequently, the mixtures were applied to a native 10% preparative PAA gel. Gel electrophoresis was run at room temperature up to 24 h. After electrophoresis, RNA was stained with ethidium bromide and visualized by UV light. To visualize the protein component of the complex, PAA gels were stained subsequently with Coomassie brilliant blue (CBB) R250.

Filter-binding assay

Twenty-microliter aliquots containing 1.25 pmol ^{32}P-labeled RNA and increasing amounts (0.2 pmol–4 nmol) of $3C^{pro}$ (10 nM–200 μM) in buffer C were incubated for 15 min at room temperature and subsequently spotted onto MF nitrocellulose filters (Millipore GmbH, Eschborn, Germany). Filters were washed with 5 mL ice-cold buffer C and dried. Radioactivity of filter-bound RNA was determined directly in a liquid scintillation counter. For each protein concentration, three to six filters were prepared. Background radioactivity was derived from assays not containing proteinase. The amount of radioactive RNA retained by the filter was plotted as fraction of RNA bound at saturation against protein concentration. Binding curves were derived by fitting the data points using the "CurveExpert" version 1.34 software (Daniel Hyams, Starkville, Mississippi). The $K_{d,app}$ was derived directly from the binding curves as the concentration of protein required for 50% saturation of binding (Kelly et al., 1976).

Circular dichroism spectroscopy

All CD spectra were recorded by a Jasco J710 spectropolarimeter equipped with a Neslab RT111 thermal controller unit. For CVB3 $3C^{pro}$, a CD spectrum was collected at 25 °C in the range of 260–190 nm using a cylindrical quartz cuvette with 1-cm path length (Jasco). A scan speed of 20 nm/min, a band width of 1 nm, and a resolution of 1 nm were used. Protein concentration was 0.885 μM as determined spectrophotometrically. The sample was dissolved in 5 mM natrium acetate buffer, pH 6.8.

For RNA, CD spectra were collected at 20 °C in the range of 360–200 nm using a cylindrical quartz cuvette with 0.1-cm path length (Jasco). A scan speed of 20 nm/min, a band width of 1 nm, a resolution of 1 nm, and three accumulations for each sample were used. RNA sample concentrations were 2.57, 1.32, 7.21, and 5 μM for the cloverleaves of HRV14, HRV14-Ins60, CVB3, and CVB3-Δ64, respectively, as determined spectrophotometrically. All samples were dissolved in a 20-mM potassium phosphate buffer, pH 6.8.

Deconvolution of the CVB3 $3C^{pro}$ CD spectrum

The obtained CVB3 $3C^{pro}$ CD spectrum was subjected to a deconvolution procedure to have an estimate of the secondary structure elements of the protein. The spectrum was deconvoluted via the neural network approach described by Böhm (1992) using the "simple" protein spectra database (13 proteins) and adding to that the spectrum reported by Wang and Johnson (2001) for HRV14 $3C^{pro}$. The neural network was trained in the 200–260 nm interval [due to the limited spectral window used by Wang and Johnson (2001) to record their spectrum] using the default parameters (learning rate = 0.015, momentum = 0.015) until the rms × 100 was below 0.086. The average error on untrained recall was 1.03%; the average error on trained recall was 1.47%.

ACKNOWLEDGMENTS

The excellent technical assistance of Sabine Wachsmuth is acknowledged. We thank Ellie Ehrenfeld, Elizabeth Hoey, Timothy Skern, and Eckard Wimmer for the gift of plasmids. This work was supported by the Deutsche Forschungsgemeinschaft (grants Ze 446/1-1 and Go 474/3-1).

Received August 10, 2001; returned for revision September 14, 2001; revised manuscript received October 26, 2001

REFERENCES

Andino R, Rieckhoff GE, Achacoso PL, Baltimore D. 1993. Poliovirus RNA synthesis utilizes an RNP complex formed around the 5′-end of viral RNA. *EMBO J 12*:3587–3598.

Andino R, Rieckhoff GE, Baltimore D. 1990a. A functional ribonucleoprotein complex forms around the 5′ end of poliovirus RNA. *Cell 63*:369–380.

Andino R, Rieckhoff GE, Trono D, Baltimore D. 1990b. Substitution on the protease ($3C^{pro}$) gene of poliovirus can suppress a mutation in the 5′ noncoding region. *J Virol 64*:607–612.

Blyn LB, Swiderek KM, Richards O, Stahl DC, Semler BL, Ehrenfeld E. 1995. Poly(rC) binding protein 2 binds to stem-loop IV of the

poliovirus RNA 5′ noncoding region: Identification by automated liquid chromatography-tandem mass spectrometry. *Proc Natl Acad Sci USA 93*:11115–11120.

Böhm G. 1992. Quantitative analysis of proteins for UV circular dichroism spectra by neural networks. *Protein Eng 5*:191–195.

Borman A, Deliat FG, Kean KM. 1994. Sequences within the poliovirus internal ribosome entry segment control viral RNA synthesis. *EMBO J 13*:3149–3157.

Gamarnik AV, Andino R. 1997. Two functional complexes formed by KH domain containing proteins with the 5′ noncoding region of poliovirus RNA. *RNA 3*:882–892.

Görlach M, Burd CG, Dreyfuss G. 1994. The mRNA poly(A)-binding protein: Localization, abundance and RNA-binding specificity. *Exp Cell Res 211*:400–407.

Grüne M, Görlach M, Soskic V, Klussmann S, Bald R, Fürste JP, Erdmann VA, Brown LR. 1996. Initial analysis of 750 MHz NMR spectra of selectively [15N]-G,U labelled *E. coli* 5S rRNA. *FEBS Lett 385*:114–118.

Hämmerle T, Molla A, Wimmer E. 1992. Mutational analysis of the proposed FG loop of poliovirus proteinase 3C identifies amino acids that are necessary for 3CD cleavage and might be determinants of a function distinct from proteolytic activity. *J Virol 66*:6028–6034.

Harris KS, Xiang W, Alexander L, Lane WS, Paul AV, Wimmer E. 1994. Interaction of poliovirus polypeptide 3CDpro with the 5′ and 3′ termini of the poliovirus genome. Identification of viral and cellular cofactors needed for efficient binding. *J Biol Chem 269*: 27004–27014.

Huang H, Alexandrov A, Chen X, Barnes TW III, Zhang H, Dutta K, Pascal SM. 2001. Structure of an RNA hairpin from HRV-14. *Biochemistry 40*:8055–8064.

Joachims M, Van Breugel PC, Lloyd RE. 1999. Cleavage of poly(A)-binding protein by enterovirus proteases concurrent with inhibition of translation in vitro. *J Virol 73*:718–727.

Johnson KH, Gray DM, Morris PA, Sutherland JC. 1990. AU and GC base pairs in synthetic RNAs have characteristic vacuum UV CD bands. *Biopolymers 29*:325–333.

Johnson VH, Semler BL. 1988. Defined recombinants of poliovirus and coxsackievirus: Sequence-specific deletions and functional substitutions in the 5′-noncoding regions of viral RNAs. *Virology 162*:47–57.

Kelly RC, Jensen DE, von Hippel PH. 1976. DNA "melting" proteins. IV. Fluorescence measurements of binding parameters for bacteriophage T4 gene 32-protein to mono-, oligo- and polynucleotides. *J Biol Chem 251*:7240–7250.

Kusov YY, Gauss-Müller V. 1997. In vitro RNA binding of the hepatitis A virus proteinase 3C (HAV 3Cpro) to secondary structure elements within the 5′-terminus of the HAV genome. *RNA 3*:291–302.

Leong LE-C, Walker PA, Porter AG. 1993. Human rhinovirus-14 protease 3C ($3C^{pro}$) binds specifically to the 5′-noncoding region of the viral RNA. *J Biol Chem 268*:25735–25739.

Lindberg AM, Crowell RL, Zell R, Kandolf R, Pettersson U. 1992. Mutations in capsid polypeptide VP2 alter the tropism of the Nancy strain of Coxsackievirus B3. *Virus Res 24*:187–196.

Matthews DA, Dragovich PS, Webber SE, Fuhrman SA, Patick AK, Zalman LS, Hendrickson TF, Love RA, Prins TJ, Marakovits JT, Zhou R, Tikhe J, Ford CE, Meador JW, Ferre RA, Brown EL, Binford SL, Brothers MA, Delisle DM, Worland ST. 1999. Structure-assisted design of mechanism-based irreversible inhibitors of human rhinovirus 3C protease with potent antiviral activity against multiple rhinovirus serotypes. *Proc Natl Acad Sci USA 96*: 11000–11007.

Mirmira SR, Tinoco I Jr. 1996. A quadruple mutant T4 RNA hairpin with the same structure as the wild-type translational repressor. *Biochemistry 35*:7675–7683.

Nicklin MJH, Harris KS, Pallai PV, Wimmer E. 1988. Poliovirus proteinase 3C: Large-scale expression, purification, and specific cleavage activity on natural and synthetic substrates in vitro. *J Virol* 62:4586–4593.

Parsley TB, Towner JS, Blyn LB, Ehrenfeld E, Semler BL. 1997. Poly (rC) binding protein 2 forms a ternary complex with the 5′-terminal sequences of poliovirus RNA and the viral 3CD proteinase. *RNA 3*:1124–1134.

Rueckert RR. 1995. Picornaviridae: The viruses and their replication. In: Fields BN, Knipe DM, Howley PM, eds. *Virology*, 3rd ed. Philadelphia: Lippincott-Raven Publishers. pp 609–654.

Ryan MD, Flint M. 1997. Virus-encoded proteinases of the picornavirus super-group. *J Gen Virol 78*:699–723.

Sprecher CA, Johnson WC Jr. 1977. Circular dichroism of nucleic acids monomers. *Biopolymers 16*:2243–2264.

Stoldt M, Wöhnert J, Görlach M, Brown LR. 1998. The NMR structure of *Escherichia coli* ribosomal protein L25 shows homology to general stress proteins and glutaminyl-tRNA synthetases. *EMBO J 17*:6377–6384.

Todd S, Towner JS, Semler BL. 1997. Translation and replication properties of the human rhinovirus genome in vivo and in vitro. *Virology 229*:90–97.

Walker PA, Leong LE, Porter AG. 1995. Sequence and structural determinants of the interaction between the 5′-noncoding region of picornavirus RNA and rhinovirus protease 3C. *J Biol Chem 270*:14510–14516.

Wang QM, Johnson RB. 2001. Activation of human rhinovirus 14 3C protease. *Virology 280*:80–86.

Xiang W, Harris KS, Alexander L, Wimmer E. 1995. Interaction between the 5′-terminal cloverleaf and 3AB/3CDpro of poliovirus is essential for RNA replication. *J Virol 69*:3658–3667.

Zell R, Klingel K, Sauter M, Fortmüller U, Kandolf R. 1995. Coxsackieviral proteins functionally recognize the polioviral cloverleaf structure of the 5′-NTR of a chimeric enterovirus RNA: Influence of species-specific host cell factors on virus growth. *Virus Res 39*:87–103.

Zell R, Sidigi K, Henke A, Schmidt-Brauns J, Hoey E, Martin S, Stelzner A. 1999. Functional features of the bovine enterovirus 5′-non-translated region, *J Gen Virol 80*:2299–2309.

Zell R, Stelzner A. 1997. Application of genome sequence information to the classification of bovine enteroviruses: The importance of 5′- and 3′-nontranslated regions. *Virus Res 51*:213–229.